

# Head to head comparison of optical coherence tomography, intravascular ultrasound echogenicity and virtual histology for the detection of changes in polymeric struts over time: insights from the ABSORB trial

Salvatore Brugaletta<sup>1,2</sup>, MD; Josep Gomez-Lara<sup>1</sup>, MD; Nico Bruining<sup>1</sup>, PhD; Maria D. Radu<sup>1</sup>, MD; Robert-Jan van Geuns<sup>1</sup>, MD, PhD; Leif Thuesen<sup>3</sup>, MD; Dougal McClean<sup>4</sup>, MD; Jacques Koolen<sup>5</sup>, MD, PhD; Stephan Windecker<sup>6</sup>, MD, PhD; Robert Whitbourn<sup>7</sup>, MD; James Oberhauser<sup>8</sup>, PhD; Richard Rapoza<sup>8</sup>, PhD; John A. Ormiston<sup>9</sup>, MBChB, PhD; Hector M. Garcia-Garcia<sup>1,10</sup>, MD, PhD; Patrick W. Serruys<sup>1\*</sup>, MD, PhD

1. Thoraxcenter, Erasmus MC, Rotterdam, The Netherlands; 2. Thorax Institute, Department of Cardiology, Hospital Clinic, Barcelona, Spain; 3. Skejby Sygehus, Aarhus University Hospital, Aarhus, Denmark; 4. Christchurch Hospital, Christchurch, New Zealand; 5. Catharina Hospital, Eindhoven, The Netherlands; 6. Bern University Hospital, Bern, Switzerland; 7. St Vincent's Hospital, Fitzroy, Australia; 8. Abbott Vascular, Santa Clara, CA, USA; 9. Auckland City Hospital, Auckland, New Zealand; 10. Cardialysis BV, Rotterdam, The Netherlands

## KEYWORDS

- virtual histology
- OCT
- imaging

## Abstract

**Aims:** To analyse and to compare the changes in the various optical coherence tomography (OCT), echogenicity and intravascular ultrasound virtual histology (VH) of the everolimus-eluting bioresorbable scaffold (ABSORB) degradation parameters during the first 12 months after ABSORB implantation. In the ABSORB study, changes in the appearance of the ABSORB scaffold were monitored over time using various intracoronary imaging modalities. The scaffold struts exhibited a progressive change in their black core area by OCT, in their ultrasound derived grey level intensity quantified by echogenicity, and in their backscattering ultrasound signal, identified as “pseudo dense-calcium” (DC) by VH.

**Methods and results:** From the ABSORB Cohort B trial 35 patients had paired OCT, echogenicity and VH assessment at baseline and at six- (n=18) or 12-months follow-up (n=17). Changes in OCT strut core area, hyperechogenicity and VH-derived DC were analysed and compared at the various time points. At six months, the change (median[IQR]) in OCT strut core area was -7.2% (-14.0-+0.9) (p=0.053), in hyperechogenicity -12.7% (-33.7-+1.4) (p=0.048) and VH-DC 22.1% (-10.8-+48.8) (p=0.102). At 12 months, all the imaging modalities showed a decrease in the various parameters considered (OCT: -12.2% [-17.5- -1.9], p=0.093; hyperechogenicity -24.64% [-36.6- -16.5], p=0.001; VH-DC: -24.66% [-32.0- -7.0], p=0.071). However, the correlation between the relative changes in these parameters was statistically poor (Spearman's rho <0.4).

**Conclusions:** OCT, echogenicity and VH were able to detect changes in the ABSORB scaffold struts, although the correlation between those changes was poor. This is likely due to the fact that each imaging modality interrogates different material properties on different length scales. Further studies are needed to explore these hypotheses.

\*Corresponding author: Erasmus MC, Thoraxcenter, 's Gravendijkwal 230, NL-3015 CE Rotterdam, The Netherlands.  
E-mail: p.w.j.serruys@erasmusmc.nl

## Abbreviations

<b>IVUS</b>	intravascular ultrasound
<b>LLI</b>	LightLab Imaging
<b>OCT</b>	optical coherence tomography
<b>PDLLA</b>	poly(D,L-lactide)
<b>PLA</b>	polylactide
<b>PLLA</b>	poly(L-lactide)
<b>VH</b>	virtual histology

## Introduction

The everolimus-eluting bioresorbable ABSORB scaffold (Abbott Vascular, Santa Clara, CA, USA) represents a novel approach for the treatment of coronary lesions, providing transient luminal support and vessel wall drug delivery without the long-term limitations of conventional metallic drug-eluting stents<sup>1-3</sup>.

In the ABSORB trials, multi-modality imaging techniques were applied, including optical coherence tomography (OCT), intravascular ultrasound (IVUS) greyscale and virtual histology (VH). These modalities have been extensively used, primarily to investigate geometric changes to the vessel wall and lumen and secondarily to assess changes in the appearance of the struts, as surrogate for changes in polymer microstructure caused by hydrolytic degradation of the polymer over time. OCT, for example, monitored the progressive integration of the scaffold into the vessel wall, with modification in the reflectivity of the strut core area and in the size of the black strut core area<sup>3,4</sup>; IVUS showed a progressive reduction in the grey level intensity of the polymeric struts over time, detected by change in hyperechogenicity<sup>5</sup>, and VH reported changes in dense calcium areas (DC) as the struts are detected by the software as “pseudo dense-calcium”<sup>2,3,6,7</sup>.

However, no systematic and serial comparison between these three intracoronary imaging modalities and their derived parameters, detecting the polymer microstructural changes, has been made. With this “pilot-study”, we tried to quantitatively compare the material property changes of the scaffold as detected by OCT, echogenicity and VH *in vivo* at six and 12 months after ABSORB implantation.

## Methods

### STUDY POPULATION

The ABSORB Cohort B study enrolled 101 patients older than 18 years of age with a diagnosis of stable/unstable angina or silent ischaemia (Trial number: NCT00856856). Those patients were divided into two groups: the first group (Cohort B1) underwent invasive imaging including greyscale IVUS, IVUS-VH and OCT at six-month follow-up; the second group (Cohort B2) had the same invasive imaging at 12 months<sup>3</sup>. All lesions were *de novo*, in a native coronary artery with a reference vessel diameter of 3.0 mm, a percentage diameter stenosis  $\geq 50\%$  and  $< 100\%$ , a thrombolysis in myocardial infarction flow grade of  $\geq 1$ , and were treated with implantation of an ABSORB scaffold (3.0×18 mm). Major exclusion criteria were: patients with an acute myocardial infarction, unstable arrhythmias or who had a left ventricular ejection fraction

$< 30\%$ , restenotic lesions, lesions located in the left main coronary artery, lesions involving a side branch  $\geq 2$  mm in diameter, and the presence of thrombus or other clinically significant stenoses in the target vessel. The local ethics committee at each participating institution approved the trial and each patient gave written informed consent before inclusion.

Only patients with paired IVUS-VH, echogenicity and OCT data were included in the present analysis.

### ABSORB SCAFFOLD

The ABSORB scaffold is a fully bioresorbable intracoronary device made from semi-crystalline poly(L-lactide) (PLLA) coated with an amorphous poly(D,L-lactide) (PDLLA) copolymer that contains and controls the release of the antiproliferative drug everolimus. The primary mechanism for molecular weight degradation of both polylactide (PLA) materials is hydrolysis, a process in which the ester bonds present in the monomeric subunit of PLA molecules are progressively cleaved. Ultimately, PLLA and PDLLA degrade to lactic acid, which is readily converted to lactate and processed via both the Krebs's cycle (for L-lactate) and methylglyoxal metabolism (for D-lactate<sup>1,2,8</sup>). Based on preclinical studies, the time for complete resorption is assumed to be approximately two years<sup>9</sup>.

The ABSORB Cohort A and Cohort B trials evaluated the ABSORB scaffold generation 1.0 and 1.1, respectively<sup>1,2</sup>. There are no differences in polymeric material, drug dose, drug release rate or strut thickness between the two generations. Of note, the ABSORB 1.1 has a smaller maximum circular unsupported surface area than the ABSORB 1.0<sup>10</sup>. Controls implemented in the manufacturing of ABSORB 1.1 have resulted in more prolonged luminal support post-implantation<sup>3</sup>.

### IVUS ACQUISITION

Treated vessels were examined post-procedure and at follow-up with 20 MHz phased array intravascular ultrasound (IVUS) Eagle-eye® catheters (Volcano Corporation, Rancho Cordova, CA, USA), using automated pullback at 0.5 mm per second after administration of 0.2 mg intracoronary nitroglycerine. IVUS analyses were performed by an independent core laboratory (Cardialysis BV, Rotterdam, The Netherlands).

### IVUS-VH ANALYSIS

Backscattering of radiofrequency signals provides information on vessel wall tissue composition<sup>11</sup>. All IVUS-VH analyses were performed offline using the pcVH 2.1 software (Volcano Corporation, Rancho Cordova, CA, USA). Four tissue components (necrotic core: red; dense calcium: white; fibrous: green; and fibrofatty: light green) were identified with autoregressive classification systems<sup>11,12</sup>. Each individual tissue component was quantified, colour coded in all IVUS cross-sections and reported as absolute and relative areas<sup>11</sup>. As previously shown, the polymeric struts are normally classified as areas of “pseudo dense calcium” (DC)<sup>2,3,6,7,13</sup>. For this reason, we assessed the change in DC areas between post-implantation and follow-up as previously reported<sup>1,2,6</sup>.

## IVUS ECHOGENICITY ANALYSIS

Fully-automated quantitative echogenicity analysis software, previously developed in-house and validated, was used to quantify the hyperechogenicity in the treated segment<sup>5,14</sup>. Briefly, the mean grey value of the adventitia is used to classify tissue components as either hypo- or hyperechogenic. The adventitia circumscribing the coronary artery is defined as a layer extending from 0.2 to 0.5 mm outside the external elastic membrane. To minimise artefacts, tissue within acoustic shadowed areas is excluded and very high grey level pixels are identified as upper tissue<sup>14</sup>. After the tissue identification process, the relative fraction of hypo- versus hyperechogenic tissue volumes are calculated for the entire scaffold segment<sup>5</sup>. As the polymeric struts, due to a high grey value intensity, are identified as hyperechogenic tissue and show a continuous decrease of their grey level intensity during the degradation process, we therefore used changes in hyperechogenicity as a surrogate for scaffold degradation, as previously described<sup>5,15,16</sup>.

## OCT ACQUISITION AND ANALYSIS

OCT imaging was performed as an optional investigation in selected centres, using either time domain (M3 system; LightLab Imaging [LLI], Westford, MA, USA) or frequency domain OCT systems (C7XR system, LLI) at baseline and follow-up<sup>10,17-21</sup>. The OCT measurements were performed with proprietary software for offline analysis (LightLab Imaging). Adjusting for the pullback speed, the analysis of continuous cross-sections was performed at 1 mm longitudinal intervals within the treated segment.

The ABSORB scaffold shows important differences with respect to metallic stents when imaged by OCT. The optically translucent polymer allows imaging of both luminal and abluminal boundaries of the strut, which appears as a box with a black central core (strut core area) framed by highly reflective borders<sup>3</sup>. The second generation ABSORB 1.1 shows, up to 12 months, a progressive decrease in strut core area, and none of the changes in morphological strut appearance that were seen with the first generation ABSORB 1.0<sup>1,2</sup>. In this analysis, we therefore focus on the changes in the strut core area between post-implantation and follow-up, as a surrogate for scaffold degradation<sup>3,4</sup>.

## STATISTICAL ANALYSIS

Categorical variables are expressed as counts and percentages. Continuous variables are presented as mean±standard deviation or median and interquartile range, according to their normal or not normal distribution. Normality of the data was evaluated using the Kolmogorov-Smirnov test. The correlation between various parameters across all time points was performed with the Spearman's test, as the data were not normally distributed.

The percentage changes for VH-derived dense calcium, hyperechogenicity and strut core area by OCT were calculated for each scaffolded coronary segment as follows:

$$\frac{(\text{Follow-up} - \text{post ABSORB scaffold implantation})}{\text{post ABSORB scaffold implantation}} \times 100\%$$

A two-tailed value of  $p < 0.05$  was considered statistically significant. Statistical analyses were performed with SPSS 16.0 software (SPSS Inc., Chicago, IL, USA).

## Results

### BASELINE CLINICAL AND ANGIOGRAPHIC CHARACTERISTICS

Overall, 35 patients had paired multi-modality imaging analyses post-implantation and at follow-up. Of these, 17 patients were followed up at six months, and the remaining 18 were followed up at 12 months. Clinical and angiographic characteristics are shown in **Table 1**.

**Table 1. Clinical and angiographic baseline characteristics.**

	Cohort B1 (n=17)	Cohort B2 (n=18)
Age (years) mean±SD (n)	61.0±9.0	60.0±9.1
Men, n (%)	13 (76)	13 (72)
Smokers, n (%)	4 (23)	5 (27)
Diabetes, n (%)	2 (12)	2 (11)
Hypertension requiring medication, n (%)	8 (47)	11 (61)
Hyperlipidaemia requiring medication, n (%)	15 (88)	11 (61)
Previous target vessel intervention, n (%)	4 (23)	3 (16)
Previous myocardial infarction, n (%)	8 (47)	2 (11)
Clinical presentation, n (%)		
Stable angina	14 (82)	13 (72)
Unstable angina	2 (12)	3 (16)
Silent ischaemia	0 (0)	2 (12)
Target vessel, n (%)		
Left anterior descending	6 (35)	11 (61)
Left circumflex	5 (30)	4 (22)
Right coronary artery	6 (35)	3 (17)
SD: standard deviation		

### MULTI-IMAGING ANALYSES FROM OCT, IVUS-VH AND ECHOGENICITY AT SIX AND 12 MONTHS

**Table 2** shows the mean strut core area, mean absolute and relative VH-DC area, mean absolute and relative hyperechogenicity values immediately after ABSORB implantation and at six and 12-month follow-up.

At six months, the change in strut core area by OCT was  $-7.25\%$  ( $-14.07$ – $+0.98$ ) ( $p=0.053$ ), in VH-DC  $22.13\%$  ( $-10.82$ – $+48.85$ ) ( $p=0.102$ ) and in hyperechogenicity  $-12.71\%$  ( $-33.70$ – $+1.41$ ) ( $p=0.048$ ). At 12 months, the change in strut core area was  $-12.20\%$  ( $-17.55$ – $-1.98$ ) ( $p=0.093$ ), in VH-DC  $-24.66\%$  ( $-32.07$ – $-7.01$ ) ( $p=0.071$ ) and in hyperechogenicity  $-24.64\%$  ( $-36.63$ – $-16.51$ ) ( $p=0.001$ ) (**Figure 1**).

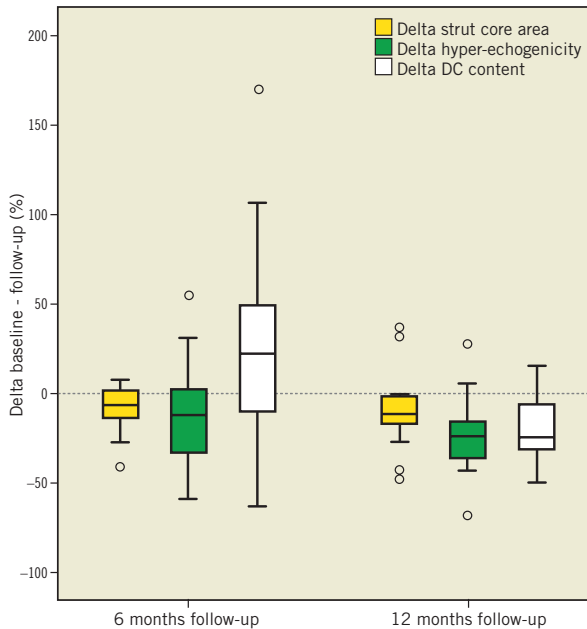
### CORRELATION BETWEEN OCT, IVUS-VH AND ECHOGENICITY

There was a poor correlation between the changes in the evaluated parameters both at six and at 12 months (six months: OCT vs. hyperechogenicity Spearman's  $\rho = -0.361$ ,  $p=0.141$ ; OCT vs. VH-DC Spearman's  $\rho = 0.362$ ,  $p=0.139$ ; hyperechogenicity vs. VH-DC Spearman's  $\rho = -0.218$ ,  $p=0.385$ ; 12 months: OCT vs.

**Table 2. Multi-imaging data from both cohorts.**

	Cohort B1 (n=17)			Cohort B2 (n=18)		
	Baseline	6-month	p-value	Baseline	12-month	p-value
Mean strut core area (mm <sup>2</sup> )	0.21±0.03	0.20±0.05	0.053	0.19±0.03	0.17±0.06	0.093
Mean DC area (mm <sup>2</sup> )	1.15±0.90	1.39±0.82	0.050	1.47±0.72	1.23±0.49	0.029
Mean DC (%)	14.10±7.08	16.27±6.67	0.102	17.38±5.62	13.75±3.92	0.071
Mean hyperechogenicity volume (mm <sup>3</sup> )	36.6±13.7	34.5±19.0	0.446	38.2±14.3	33.2±41.0	0.093
Mean hyperechogenicity (%)	23.1±9.4	19.2±8.9	0.048	24.4±10.5	18.2±8.9	0.001

DC: dense calcium

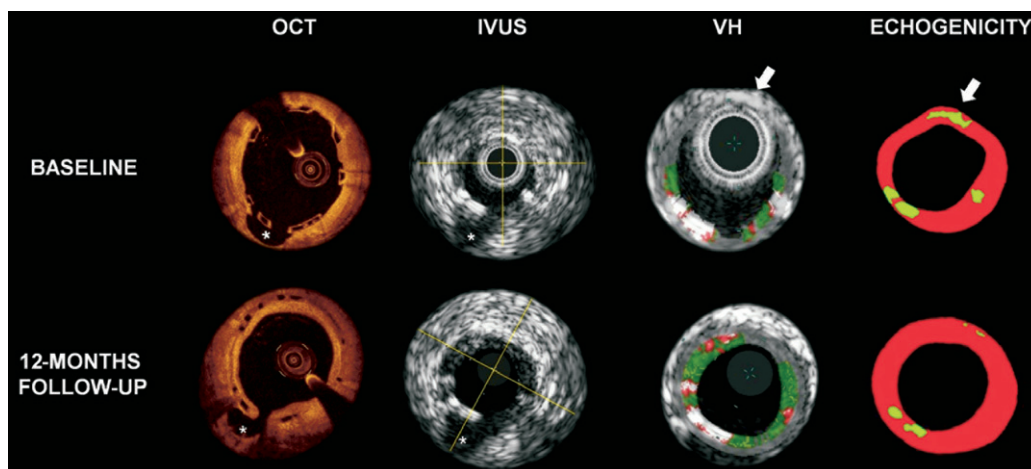
**Figure 1.** Relative reduction in strut core area, hyperechogenicity and DC content between baseline and 6/12 months follow-up. DC: dense calcium

hyperechogenicity Spearman's  $\rho=0.262$ ,  $p=0.309$ ; OCT vs. VH-DC Spearman's  $\rho=0.233$ ,  $p=0.368$ ; hyperechogenicity vs. VH-DC Spearman's  $\rho=0.368$ ,  $p=0.233$ ). The correlation did not improve when considering the data from six and 12 months together (OCT vs. hyperechogenicity Spearman's  $\rho=-0.038$ ,  $p=0.830$ ; OCT vs. VH-DC Spearman's  $\rho=0.281$ ,  $p=0.102$ ; hyperechogenicity vs. VH-DC Spearman's  $\rho=0.071$ ,  $p=0.683$ ) (Figure 2).

## Discussion

The main findings of the analysis are: 1) there appears to be a reduction in strut core area by OCT and in hyperechogenicity values both at six and 12-month follow-up; 2) VH detects contrasting changes in dense-calcium between six and 12 months; 3) at the patient level, the correlation between the various parameters detected by the three imaging modalities is poor.

One of the most interesting concepts of the ABSORB scaffold is the temporary lumen scaffolding: in contrast with metallic stents, the polymeric scaffold does not involve a permanent caging of the vessel, as it is bioresorbed over time<sup>22,23</sup>. In keeping with this concept, much interest has been focused on the use of intracoronary imaging techniques and their capabilities in detecting *in vivo* changes in scaffold material properties.

**Figure 2.** Examples of OCT, IVUS, VH and echogenicity findings of corresponding cross-sectional images with a side branch (\*) selected as an anatomical landmark. The white arrows indicate a hyperechogenic tissue in echogenicity analysis, hidden by the grey media stripe in the VH analysis. OCT: optical coherence tomography; IVUS: intravascular ultrasound; VH: virtual histology

With regard to OCT, it is sensitive to refractive index changes on a length scale greater than the wavelength of the light emitted from the catheter. For this reason, it detects the polymeric struts as being highly reflective compared to the lumen and the vessel wall. Conversely, the black strut core area, despite the heterogeneity of the semi-crystalline polymer structure, has a light-poor signal after ABSORB implantation, indicating that changes in refractive index occur on a length scale less than that of the wavelength of the OCT light. However, as hydrolytic degradation progresses, it is reasonable to expect that this polymer microstructural heterogeneity coarsens, leading eventually to an increase in OCT reflectivity. For example, in the ABSORB Cohort A trial, testing the first generation ABSORB device, OCT showed that at six months, only 3% of the strut boxes kept the so-called “preserved box” appearance seen at post-implantation, whereas the remaining 97% changed their reflectivity, becoming “open box, dissolved bright box or dissolved black box”. Each of these OCT appearances was related to different histological characteristics in an animal study, where it was shown that reduction in strut core area and transition from preserved to open/dissolved box may represent indirect signs of scaffold degradation (e.g., polymer microstructural heterogeneity) and integration into the vessel wall<sup>9</sup>. Conversely, in the ABSORB Cohort B trial, using the second generation ABSORB device, the scaffold struts maintained the OCT-defined “preserved box” appearance both at six and at 12-month follow-up exhibiting a progressive reduction in black strut core area by OCT<sup>3,24</sup>. Concomitantly, IVUS greyscale showed a progressive reduction in the grey level intensity of the struts; this phenomenon was quantified by echogenic analysis, demonstrating a reduction in the hyperechogenicity values of the polymeric struts over time<sup>5</sup>. In the ABSORB Cohort A study, quantitative differential echogenicity was already applied to monitor *in vivo* changes of the scaffold by means of the acoustic property changes, showing an increase of hyperechogenic tissue immediately after the ABSORB implantation, which was back to pre-implantation values at the time of expected degradation and bioresorption (approximately two years<sup>2,5</sup>). At six months, the differences in hyperechogenic reduction between the ABSORB Cohort A and Cohort B (50% vs. 17%) were in line with the differences in the struts’ OCT appearance and in the late loss (0.43 mm vs. 0.19 mm), further supporting differences in hydrolytic degradation rate characteristics between the two ABSORB devices<sup>3</sup>.

At variance with these findings, a slight increase in the backscattering signal of the struts interpreted as dense calcium by VH was detected at six months with a subsequent decrease at 12 months. It should be kept in mind that not only the polymeric scaffold –with its presence and degradation– but also the tissue surrounding the struts contributes to the VH-derived dense calcium quantification, which may explain this contrasting finding<sup>6,25</sup>. In particular, our global evaluation of the area comprised between the lumen and the medial stripe integrates into our quantification of dense calcium also the backscattering signal not related to the sole struts, but, for instance, to the plaque behind the scaffold. Changes in composition of this plaque are therefore also detected by VH. In a porcine model

some inflammatory cells, such as granuloma and giant cells, were found surrounding the polymeric struts in the early stages after implantation, before decreasing over time<sup>9</sup>. At six months, focusing on the VH appearance of the plaque behind the scaffold, we confirmed this observation in humans, finding a progression in the NC content<sup>25</sup>. Of note is that dense calcium is a frequent finding within the necrotic core region; in this case it is frequently “speckled” and can be due to calcification of a “nidus” of macrophages<sup>26</sup>. Changes over time in strut core area and in hyperechogenicity are instead probably less related to the plaque changes.

It is important to highlight that despite an overall agreement between hyperechogenicity and strut core area in terms of reduction of both parameters during the first 12 months, analysis at the patient level revealed that the correlation between these imaging parameters is poor. This is not surprising, since the optical and ultrasonic parameters reflect different aspects of scaffold degradation. From our animal experience, we learnt that the polymer is first hydrolysed into small oligomers digested by macrophages and that the strut voids initially occupied by the polymeric struts are then filled with proteoglycan and eventually integrated into the vessel wall. Hence, the changes in black strut core area by OCT do not reflect the molecular dissolution of the polylactide, as the polymer and the proteoglycan material have the same optical properties, but rather the filling of the strut voids by connective tissue ultimately making the struts undetectable by OCT and in histology<sup>9</sup>. Conversely, changes in the material properties of polylactide (e.g., crystallinity, molecular weight, stiffness, etc.) have previously been demonstrated to predominantly affect the acoustic properties of the material over time, and these can be detected by ultrasonic waves<sup>15,16</sup>.

Although both echogenicity and VH data are based on the application of ultrasound, the correlation between them was also poor. This lack of correlation may be explained by the differences of methodologies used in these two techniques. Whilst the echogenicity software analyses the complete image and the echo intensity (envelope amplitude), which is normally used in the formation of the greyscale-IVUS image, the VH software analyses the frequency of the signal underlying the amplitude (radiofrequency backscattering). As the classification tree of VH was not validated for recognition of metallic/polymeric struts, the backscattering signal, derived from a stent/scaffold, was usually interpreted by the software as dense calcium, such as found in heavily calcified coronary segments<sup>6,27</sup>. Conversely, echogenicity analysis excluded from its tissue quantification the acoustically shadowed areas, resulting in a likely better discrimination between polymeric struts and calcified coronary segments. Another important point to consider in the VH detection of the polymeric struts is that some scaffold strut information may be missed because of the presence of the medial grey stripe and it is extremely dependent on the contours drawing<sup>28,29</sup> (**Figure 2**). In addition no data are available to date correlating the backscattering signal changes with the physical and mechanical properties of polylactide.

Finally, it is important to note the difference in variability of the various changes explored by these techniques, with OCT exhibiting

the least variability (**Figure 1**). The fundamental differences in the principles and spatial resolution of each technique should be taken into account in the interpretation of this variability and also of their poor correlation<sup>30,31</sup>.

## Limitations

A major limitation of our analysis is the small number of patients compared to the total number of patients enrolled in the trial. For this reason the p-values of the modification over time in the various parameters investigated have to be considered as exploratory. Nevertheless, limiting the analysis to only patients receiving all three imaging modalities allows a more accurate comparison between the various parameters investigated. Lack of data about the polylactide degradation has also to be taken into account as a possible limitation of our comparison. An *in vitro* or *ex vivo* study would be required to correlate these parameters with the scaffold/polymer degradation.

## Conclusions

Our analysis showed that during the first 12 months after ABSORB scaffold implantation there is a reduction in black strut core area, as measured by OCT, and in the hyperechogenicity of the scaffold, representing independent signs of scaffold/polymer degradation. In contrast, VH only showed a reduction in “pseudo dense-calcium” at 12 months indicating some limitations in monitoring scaffold property changes.

## Acknowledgements

The ABSORB Trial is sponsored and funded by Abbott Vascular, Santa Clara, CA, USA.

## Conflict of interest statement

J. Oberhauser and R. Rapoza are employees of Abbott Vascular. None of the other authors have conflicts of interest relevant to the subject material in this paper.

## References

1. Ormiston JA, Serruys PW, Regar E, Dudek D, Thuesen L, Webster MW, Onuma Y, Garcia-Garcia HM, McGreevy R, Veldhof S. A bioabsorbable everolimus-eluting coronary stent system for patients with single de-novo coronary artery lesions (ABSORB): A prospective open-label trial. *Lancet*. 2008;371:899-907.
2. Serruys PW, Ormiston JA, Onuma Y, Regar E, Gonzalo N, Garcia-Garcia HM, Nieman K, Bruining N, Dorange C, Miquel-Hebert K, Veldhof S, Webster M, Thuesen L, Dudek D. A bioabsorbable everolimus-eluting coronary stent system (ABSORB): 2-year outcomes and results from multiple imaging methods. *Lancet*. 2009;373:897-910.
3. Serruys PW, Onuma Y, Ormiston JA, de Bruyne B, Regar E, Dudek D, Thuesen L, Smits PC, Chevalier B, McClean D, Koolen J, Windecker S, Whitbourn R, Meredith I, Dorange C, Veldhof S, Miquel-Hebert K, Rapoza R, Garcia-Garcia HM. Evaluation of the second generation of a bioresorbable everolimus drug-eluting vas-

cular scaffold for treatment of de novo coronary artery stenosis: Six-month clinical and imaging outcomes. *Circulation*. 2010;122:2301-2312.

4. Gomez-Lara J, Brugaletta S, Diletti R, Garg S, Onuma Y, Gogas BD, van Geuns RJ, Dorange C, Veldhof S, Rapoza R, Whitbourn R, Windecker S, Garcia-Garcia HM, Regar E, Serruys PW. A comparative assessment by optical coherence tomography of the performance of the first and second generation of the everolimus-eluting bioresorbable vascular scaffolds. *Eur Heart J*. 2011;32:294-304.

5. Bruining N, de Winter S, Roelandt JR, Regar E, Heller I, van Domburg RT, Hamers R, Onuma Y, Dudek D, Webster MW, Thuesen L, Ormiston JA, Cheong WF, Miquel-Hebert K, Veldhof S, Serruys PW. Monitoring in vivo absorption of a drug-eluting bioabsorbable stent with intravascular ultrasound-derived parameters a feasibility study. *JACC Cardiovasc Interv*. 2010;3:449-456.

6. Garcia-Garcia HM, Gonzalo N, Pawar R, Kukreja N, Dudek D, Thuesen L, Ormiston JA, Regar E, Serruys PW. Assessment of the absorption process following bioabsorbable everolimus-eluting stent implantation: Temporal changes in strain values and tissue composition using intravascular ultrasound radiofrequency data analysis. A substudy of the ABSORB clinical trial. *EuroIntervention*. 2009;4:443-448.

7. Brugaletta S, Garcia-Garcia HM, Diletti R, Gomez-Lara J, Garg S, Onuma Y, Shin ES, Van Geuns RJ, De Bruyne B, Dudek D, Thuesen L, Chevalier B, McClean D, Windecker S, Whitbourn R, Dorange C, Veldhof S, Rapoza R, Sudhir K, Bruining N, Ormiston J, Serruys P. Comparison between the first and second generation bioresorbable vascular scaffolds: A six month virtual histology study. *EuroIntervention*. 2011;6:1110-6.

8. Ewaschuk JB, Naylor JM, Zello GA. D-lactate in human and ruminant metabolism. *J Nutr*. 2005;135:1619-1625.

9. Onuma Y, Serruys PW, Perkins LE, Okamura T, Gonzalo N, Garcia-Garcia HM, Regar E, Kamberi M, Powers JC, Rapoza R, van Beusekom H, van der Giessen W, Virmani R. Intracoronary optical coherence tomography and histology at 1 month and 2, 3, and 4 years after implantation of everolimus-eluting bioresorbable vascular scaffolds in a porcine coronary artery model: An attempt to decipher the human optical coherence tomography images in the ABSORB trial. *Circulation*. 2010;122:2288-2300.

10. Okamura T, Garg S, Gutierrez-Chico JL, Shin ES, Onuma Y, Garcia HM, Rapoza R, Sudhir K, Regar E, Serruys PW. In vivo evaluation of stent strut distribution patterns in the bioabsorbable everolimus-eluting device: an OCT ad hoc analysis of the revision 1.0 and revision 1.1 stent design in the ABSORB clinical trial. *EuroIntervention*. 2010;6:932-938.

11. Nair A, Kuban BD, Tuzcu EM, Schoenhagen P, Nissen SE, Vince DG. Coronary plaque classification with intravascular ultrasound radiofrequency data analysis. *Circulation*. 2002;106:2200-2206.

12. Nasu K, Tsuchikane E, Katoh O, Vince DG, Virmani R, Surmely JF, Murata A, Takeda Y, Ito T, Ehara M, Matsubara T, Terashima M, Suzuki T. Accuracy of in vivo coronary plaque morphology assessment: A validation study of in vivo virtual histology

compared with in vitro histopathology. *J Am Coll Cardiol.* 2006;47:2405-2412.

13. Serruys PW, Onuma Y, Dudek D, Smits PC, Koolen J, Chevalier B, De Bruyne B, Thuesen L, McClean D, van Geuns RJ, Windecker S, Whitbourn R, Meredith C, Dorange C, Veldhof S, Miquel-Hebert K, Sudhir K, Garcia-Garcia HM, Ormiston JA. Evaluation of the second generation of a bioresorbable everolimus-eluting vascular scaffold for the treatment of de novo coronary artery stenosis: 12-month clinical and imaging outcomes. *J Am Coll Cardiol.* 2011;58:1578-88.

14. Bruining N, Verheye S, Knaapen M, Somers P, Roelandt JR, Regar E, Heller I, de Winter S, Ligthart J, Van Langenhove G, de Feijter PJ, Serruys PW, Hamers R. Three-dimensional and quantitative analysis of atherosclerotic plaque composition by automated differential echogenicity. *Catheter Cardiovasc Interv.* 2007;70:968-978.

15. Wu HC, Shen FW, Hong X, Chang WV, Winet H. Monitoring the degradation process of biopolymers by ultrasonic longitudinal wave pulse-echo technique. *Biomaterials.* 2003;24:3871-3876.

16. Parker NG, Mather ML, Morgan SP, Povey MJ. Longitudinal acoustic properties of poly(lactic acid) and poly(lactic-co-glycolic acid). *Biomed Mater.* 2010;5:055004.

17. Sihan K, Botha C, Post F, de Winter S, Gonzalo N, Regar E, Serruys PJ, Hamers R, Bruining N. Fully automatic three-dimensional quantitative analysis of intracoronary optical coherence tomography: Method and validation. *Catheter Cardiovasc Interv.* 2009;74:1058-1065.

18. Prati F, Regar E, Mintz GS, Arbustini E, Di Mario C, Jang IK, Akasaka T, Costa M, Guagliumi G, Grube E, Ozaki Y, Pinto F, Serruys PW. Expert review document on methodology, terminology, and clinical applications of optical coherence tomography: Physical principles, methodology of image acquisition, and clinical application for assessment of coronary arteries and atherosclerosis. *Eur Heart J.* 2010;31:401-415.

19. Gonzalo N, Serruys PW, Okamura T, Shen ZJ, Onuma Y, Garcia-Garcia HM, Sarno G, Schultz C, van Geuns RJ, Ligthart J, Regar E. Optical coherence tomography assessment of the acute effects of stent implantation on the vessel wall: A systematic quantitative approach. *Heart.* 2009;95:1913-1919.

20. Regar E, Leeuwen AMGJv, Serruys PW. Optical coherence tomography in cardiovascular research. *Informa Healthcare;* 2007.

21. Gonzalo N, Serruys PW, Garcia-Garcia HM, van Soest G, Okamura T, Ligthart J, Knaapen M, Verheye S, Bruining N, Regar E. Quantitative ex vivo and in vivo comparison of lumen dimensions

measured by optical coherence tomography and intravascular ultrasound in human coronary arteries. *Rev Esp Cardiol.* 2009;62:615-624.

22. Onuma Y, Serruys PW. Bioresorbable scaffold: The advent of a new era in percutaneous coronary and peripheral revascularization? *Circulation.* 2011;123:779-797.

23. Oberhauser JP, Hossainy S, Rapoza R. Design principles and performance of bioresorbable polymeric vascular scaffolds. *EuroIntervention.* 2009;5:F15-F22.

24. Brugaletta S, Garcia-Garcia HM, Garg S, Gomez-Lara J, Diletti R, Onuma Y, van Geuns RJ, McClean D, Dudek D, Thuesen L, Chevalier B, Windecker S, Whitbourn R, Dorange C, Miquel-Hebert K, Sudhir K, Ormiston JA, Serruys PW. Temporal changes of coronary artery plaque located behind the struts of the everolimus eluting bioresorbable vascular scaffold. *Int J Cardiovasc Imaging.* 2011;27:859-866.

25. Garcia-Garcia HM, Mintz GS, Lerman A, Vince DG, Margolis MP, van Es GA, Morel MA, Nair A, Virmani R, Burke AP, Stone GW, Serruys PW. Tissue characterisation using intravascular radiofrequency data analysis: Recommendations for acquisition, analysis, interpretation and reporting. *EuroIntervention.* 2009;5:177-189.

26. Kubo T, Maehara A, Mintz GS, Garcia-Garcia HM, Serruys PW, Suzuki T, Klauss V, Sumitsuji S, Lerman A, Marso SP, Margolis MP, Margolis JR, Foster MC, De Bruyne B, Leon MB, Stone GW. Analysis of the long-term effects of drug-eluting stents on coronary arterial wall morphology as assessed by virtual histology intravascular ultrasound. *Am Heart J.* 2010;159:271-277.

27. Shin ES, Garcia-Garcia HM, Garg S, Ligthart J, Thuesen L, Dudek D, Ormiston JA, Serruys PW. Assessment of the serial changes of vessel wall contents in atherosclerotic coronary lesion with bioresorbable everolimus-eluting vascular scaffolds using shin's method: An IVUS study. *Int J Cardiovasc Imaging.* 2011;27:931-7.

28. Mintz GS, Nissen SE, Anderson WD, Bailey SR, Erbel R, Fitzgerald PJ, Pinto FJ, Rosenfield K, Siegel RJ, Tuzcu EM, Yock PG. American college of cardiology clinical expert consensus document on standards for acquisition, measurement and reporting of intravascular ultrasound studies (ivus). A report of the american college of cardiology task force on clinical expert consensus documents. *J Am Coll Cardiol.* 2001;37:1478-1492.

29. Bezerra HG, Costa MA, Guagliumi G, Rollins AM, Simon DI. Intracoronary optical coherence tomography: A comprehensive review clinical and research applications. *JACC Cardiovasc Interv.* 2009;2:1035-1046.